Laser and Particle Beams (2011), *29*, 437–446.

doi:10.1017/S0263034611000553

Comparison of femtosecond laser-driven proton acceleration using nanometer and micrometer thick target foils

M. SCHNÜRER,[1] A.A. ANDREEV,[1,2] S. STEINKE,[1] T. SOKOLLIK,[1,3,4] T. PAASCH-COLBERG,[5] P.V. NICKLES,[6] A. HENIG,[5,7] D. JUNG,[5,7] D. KIEFER,[5,7] R. HÖRLEIN,[5,7] J. SCHREIBER,[5,7] T. TAJIMA,[5,8] D. HABS,[5,7] AND W. SANDNER[1,9]

[1]Max-Born-Institut, Berlin, Germany
[2]STC "Vavilov State Optical Institute," St. Petersburg, Russia
[3]Lawrence Berkeley National Laboratory, Berkeley, California
[4]University of California, Berkeley, California
[5]Max-Planck-Institut für Quantenoptik, Garching, Germany
[6]Gwangju Institute of Science and Technology, GIST, Republic of Korea
[7]Department für Physik, Ludwig-Maximilians-Universität München, Garching, Germany
[8]Photomedical Research Center, JAEA, Kyoto, Japan
[9]Technische Universität Berlin, Berlin, Germany

(RECEIVED 18 March 2011; ACCEPTED 25 August 2011)

Abstract

Advancement of ion acceleration by intense laser pulses is studied with ultra-thin nanometer-thick diamond like carbon and micrometer-thick Titanium target foils. Both investigations aim at optimizing the electron density distribution which is the key for efficient laser driven ion acceleration. While recently found maximum ion energies achieved with ultra-thin foils mark record values micrometer thick foils are flexible in terms of atomic constituents. Electron recirculation is one prerequisite for the validity of a very simple model that can approximate the dependence of ion energies of nanometer-thick targets when all electrons of the irradiated target area interact coherently with the laser pulse and Coherent Acceleration of Ions by Laser pulses (CAIL) becomes dominant. Complementary experiments, an analytical model and particle in cell computer simulations show, that with regard to ultra-short laser pulses (duration ~45 fs at intensities up to 5×10^{19} W/cm^2) and a micrometer-thick target foil with higher atomic number a close to linear increase of ion energies manifests in a certain range of laser intensities.

Keywords: Coherent acceleration of ions by laser pulses; Laser ion acceleration; Radiation pressure; Relativistic laser intensity; Target normal sheath acceleration

INTRODUCTION

The recent interest in the field of fast ion generation by the interaction of very intense laser pulses with matter is based on two aspects. First, processes of energy dissipation from a high energy density state that comprises fundamental processes in plasma physics together with their specific parameters has to be considered. And second, the formation of fast ion bunches emerging from a specific plasma state itself needs to be studied. It has turned out that these laser driven ion bunches have first of all a very low emittance (Cowan *et al.*, 2004), which is the unprecedented property in comparison to ion bunches being produced by a low temperature plasma source and following acceleration in a high-frequency driven cavity. The low emittance was directly exploited in several experiments where those ions have been used to image strong electric and magnetic fields in plasmas (MacKinnon *et al.*, 2004; Borghesi *et al.*, 2005; Romagnani *et al.*, 2005; Sokollik *et al.*, 2009; Willingale *et al.*, 2010).

Another conceptual advantage of the laser-ion-accelerator over conventional accelerators lies in the fact that the acceleration takes place over a distance of only several micrometers and the energy is transferred through processes at extremely high power density. To transfer the energy of the laser pulse effectively to the kinetic energy of the ions, the

Address correspondence and reprint requests to: Matthias Schnürer, Max-Born-Institut, Max-Born-Straße 2a, 12489 Berlin, Germany. E-mail: schnuerer@mbi-berlin.de

phase of the laser field, plasma electron motion, and subsequently the displacement of the ions have to be matched, which generally manifests in the coherence of the electron motion with respect to the laser field (Yan *et al.*, 2008; Tajima *et al.*, 2009) or leads in a more specific case of circular laser polarization, to the concept of dominant Radiation Pressure Acceleration (Macchi *et al.*, 2009). This phase-stable acceleration requires an accurate adjustment of the target density but very recently proton energies of 13 MeV and carbon ion energies of 70 MeV have been obtained with laser irradiated foils having a thickness of only a few nanometers. This energy increase in comparison to irradiated micrometer thick foils was accompanied by an increase of the conversion efficiency by two orders of magnitude (Steinke *et al.*, 2010). While a linear scaling of ion energies with laser intensity seems to exist in the limited range of parameters exploited by this experiment a much more extended extrapolation imposes several questions. This is mainly due to the fact that the realized scenario requires a certain density of the target as a function of the laser intensity which is connected to the onset of transparency (Henig *et al.*, 2009*a*) for the laser pulse.

Ion acceleration by lasers offers new design flexibility and would allow new concepts of ion accelerators if the ion bunch parameter can be brought in a stable manner to those measures relevant for application in e.g., material-science or biology. While tumor therapy is aiming for proton energies in a range of 200 MeV or around 80 MeV (Weichsel *et al.*, 2008), values that have not been demonstrated with lasers so far, projects have been started to utilize an energy range between 10 and 20 MeV (Kraft *et al.*, 2010).

In this paper, we discuss results of ion acceleration experiments with foil-targets of micrometer down to nanometer thickness. The comparison of different foil types includes maximum accessible ion energies for specific laser parameter and it shows to which extend a special target technology in combination with laser technology pays off. Such a consideration is necessary if a complex laser-plasma acceleration stage is designed as an ion source for application. The scaling of the ion energy as a function of target thickness and as a function of laser energy is discussed with the help of analytical models and in the case of micrometer thick foils with particle in cell (PIC) simulations. Here we show that even within the "conventional" target normal sheath acceleration (TNSA)-regime a linear increase of ion energy with laser energy is possible, an aspect that has recently also been studied elsewhere (Zeil *et al.*, 2010; Brenner *et al.*, 2011). The results are used to suggest extrapolation to moderately higher ion energies.

EXPERIMENT

Experiments have been conducted with the MBI Ti:sapph high-field-laser system. It delivers ultra-short laser pulses with 45 fs FWHM duration at 810 nm central wavelength with energy of 1.2 J on target. The laser pulse is focused onto the target with an $f = 150$ mm parabolic mirror at $f/2.5$. In different experimental runs, peak intensities between $(3–5) \times 10^{19}$ W/cm^2 have been calculated from focal spot measurements and the energy content inside the focus diameter. Focus diameters were about 4–5 μm. Different values of the temporal pulse contrast were employed. At the output of the pulse compressor, the laser system delivers an amplified spontaneous emission contrast ratio larger than 1:10^7 up to 10 ps prior to the arrival of the main peak. This contrast was increased by an estimated four orders of magnitude (Levy *et al.*, 2007) by means of a recollimating double plasma mirror (DPM) (Andreev *et al.*, 2009). The DPM pulse energy throughput was about 60–65% leading to intensities up to 5×10^{19} W/cm^2 with a focal spot size of 3.6 μm. The ultra-high contrast suppresses pre-heating and a strong expansion of the target due to the pulse background, which is a necessary prerequisite for experiments with targets at nanometer extension. Ion bunches were detected with a MCP coupled to a Thomson-Parabola spectrometer (Ter-Avetisyan *et al.*, 2005).

In order to gather additional data to benchmark our models, we performed experiments where we can directly compare the influence of a certain plasma gradient on the ion acceleration. The plasma gradient can be directly steered with the level of the pre-pulse pedestal. The best direct comparison is to switch the system inherent pre-pulse pedestal off using a DPM, which changes the intensity contrast (ratio of pedestal intensity to peak intensity) from 10^{-7}–10^{-8} (medium contrast = mc) to 10^{-11}–10^{-12} (ultra high contrast = uhc). The intensity level and duration of about 1 ns of the pulse pedestal (mc-case) is determined from measurements with a third order correlator and fast photodiodes. Values of the uhc-case are extrapolated from published performance data of DPMs and it can be assumed that the pedestal at low intensity extends to a few picoseconds in front of the pulse peak. Target foils are irradiated at 45° incidence to the target normal or close to normal incidence. At 45° irradiation, the ion emission along the target normal was registered with two spectrometers. One spectrometer recorded the ions accelerated from the laser irradiated front side (fs — spectrum) of the target and the second spectrometer the ions from the target back side (bs — spectrum).

Metal (Ti) foil targets of several μm thickness and diamond like carbon (DLC) targets of thicknesses ranging from 2.9–50 nm were employed. The DLC-foils have been produced at LMU-Munich/MPQ-Garching and they are characterized by a density of 2.7 g/cm^3 and 75% fraction of sp^3 — bonds which lead to mechanically stable, ultra-thin, free standing targets with an exceptionally high tensile strength, hardness and heat resistance. We refer to a thickness of the foils, which contains the DLC bulk together with a 1 nm hydrocarbon contamination layer on each side. The thickness was characterized by means of an atomic force microscope.

SCALING OF PROTON ENERGIES AS A FUNCTION OF TARGET THICKNESS IN CASE OF DRIVING LASER PULSES WITH ULTRA-HIGH TEMPORAL CONTRAST

Prerequisites of a simple model for ion acceleration with ultra-thin foil targets

The present concept (as e.g., TNSA (Hatchett *et al.*, 2000)) for laser driven ion acceleration is based on the creation of a strong electric field at a matter-vacuum interface. Alternatively, a direct acceleration of ions by the laser pulse as it is possible with electrons needs laser intensities of about 10^{24} W/cm^2 (Esirkepov *et al.*, 2006), which are not yet accessible in a practical manner. Therefore a series of studies are devoted to finding target and laser pulse parameter that increase the conversion of laser energy to kinetic energy of fast ions. The TNSA-concept leads consequently to the question of how a maximum charge separation can be established at a matter-vacuum interface. It has been found (Esirkepov *et al.*, 2006; Klimo *et al.*, 2008) that optimum polarization conditions can be achieved if the light pressure balances the electrostatic pressure, which arises due to charge separation and therefore depends on the charge density and laser intensity. In case of an irradiated foil, this criterion $a \sim n_e/n_c\ d_t/\lambda_L$ gives an optimum for the foil thickness d_t, where a, n_e, n_c, λ_L are the relativistically normalized laser vector potential, the electron density, the critical electron density, and the laser wavelength, respectively (cf. also Appendix). At the optimum charge separation also the highest field strength occurs and ions with the highest cut-off energies appear. This has been recently demonstrated in several experiments (Steinke *et al.*, 2010; Henig *et al.*, 2009*b*). In addition to the development of comprehensive models (Yan *et al.*, 2008; Tajima *et al.*, 2009; Macchi *et al.*, 2009; Yan *et al.*, 2010; Pae *et al.*, 2011; Andreev *et al.*, 2010), we trace the experimental findings with a very simple model that calculates the electron density and hence the ion energy as a function of the target thickness. The purpose of the simple model is to show how electron displacement can account for the experimental data.

The background of the scaling model will be described in the following whereas technical details, used equations, free parameters etc., are listed in the Appendix. The electron reservoir is determined by the ionized skin layer and the laser illuminated area of the target foil. An average charge state is assumed. Within the duration τ_L of the laser pulse electrons are produced and accelerated. They form an electron bunch with a length of approximately $\tau_L c$. The electrons of the bunch are distributed along a length THAT corresponds to the thickness of the target plus the Debye lengths of the sheath regions at the target front and rear side. Due to the electron movement they are "recirculating" between front and rear side. For our pulse, duration of 45 fs, the bunch length corresponds to about 13 micrometer and recirculation works for target foils with a thickness of up to a few micrometer. Furthermore, the electrons do not disappear immediately after termination of the laser pulse. They continue to circulate, cool down and fast ion acceleration at the target front, and rear side will cease at about 200 fs (Andreev *et al.*, 2009). This time is suggested by two-dimensional PIC simulations. Thus, the recirculation process (Steinke *et al.*, 2011) provides a certain electron density in the sheath region for some time. In the simple model discussed here, the electron — recirculation mode (Andreev *et al.*, 2009) is used to distribute the electrons equally in the target volume and the two Debye sheaths.

Experimental verification of electron recirculation

The ion emission from the target surface is a function of the electron density and its gradient. By measuring the ion emission from the target front and rear side, differences in the electron distribution can be detected. A symmetric distribution on both target sides can serve as an indicator for electron recirculation that favors such a situation. In order to do so, the target is turned to a 45° angle of laser beam incidence. This allows coincidental registration of ion emission along the target normal from front and rear side.

Figure 1 visualizes this situation for a 5 nm DLC-foil irradiated with uhc laser pulses. We also checked the drop in ion energy with decreasing intensity when the irradiation angle is switched from 0 to 45°, which is necessary for the observation of front and rear target sides in our experiment. Observation and ion recording is along the target normal.

The same situation has also been examined with targets of micrometer thickness when the temporal pulse contrast is at ultra-high and medium level. The obtained ion spectra from a Ti-foil with a thickness of 5 μm for the two different contrast ratios are shown in Figure 2. In the case of the Ti targets, the combination of target thickness and the mc is sufficient to avoid deterioration of the steep density gradient at the target rear side caused by shock — or heat waves from the irradiated front side.

The influence of the density gradient on the attainable ion energies in a TNSA-regime has been intensively discussed in several works (Zeil *et al.*, 2010; Kaluza *et al.*, 2004; Neely *et al.*, 2006; McKenna *et al.*, 2008; Flacco *et al.*, 2010; Badziak *et al.*, 2010). This influence is immediately visible when comparing the fs — and bs — spectra of Figure 2a. Preplasma expansion at the front side causes a flattened density gradient and as a result reduces the field strength of the sheath field. Consequently, the ion energies are lower compared to the ones originating from the rear side.

The two, almost identical fs — and bs — spectra in Figure 2b give rise to this scenario when an identical plasma gradient is present at target front and back side, initiated by an uhc laser pulse. In the experiment, the relation between fs- and bs-spectra concerning shape, proton numbers and cut-off values were reproducible. The absolute values changed from shot to shot within 20%, which we attribute to fluctuation of the laser irradiation conditions. From

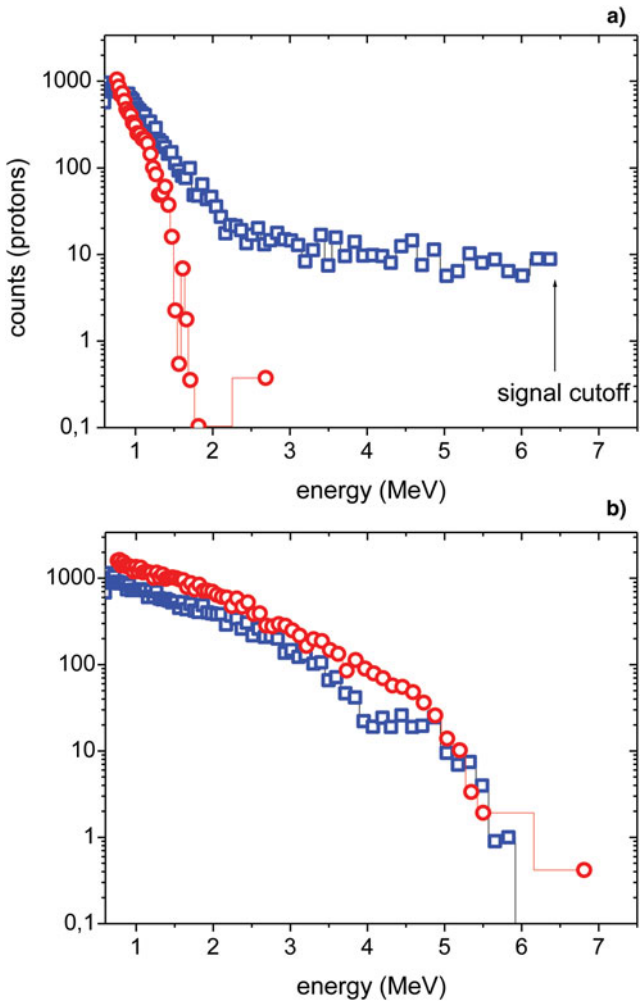

Fig. 1. (Color online) Front side (fs = red circle) and back side (bs = blue square) proton spectra obtained from laser driven Ti-foils when the intense driving laser pulse has a medium contrast (mc) pedestal pre-pulse (**a**) and an ultra-high contrast (uhc) pedestal prepulse (**b**) (parameter cf. text).

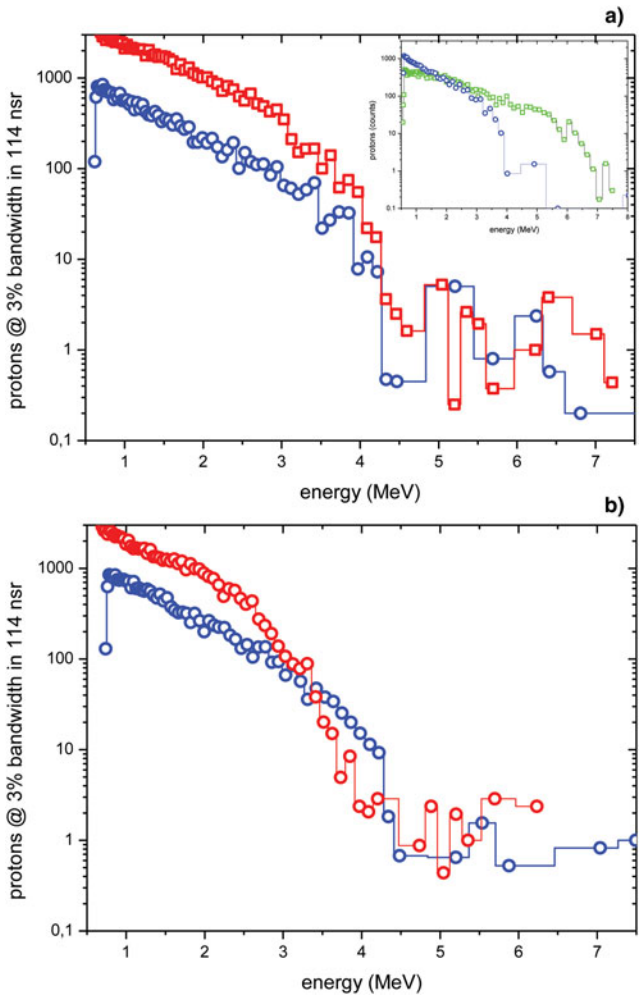

Fig. 2. (Color online) (**a**) proton emission from a 5 nm DLC-foil (red squares — protons from laser irradiated front side, blue circles — protons from target rear side) with laser irradiation at 45° to target normal, inset: proton emission from target rear side with laser irradiation at 45° to target normal (blue curve) in comparison to emission with laser irradiation at normal incidence (green curve); (**b**) similar to (a) but laser polarization was circular instead of linear.

the similarity of the electron distribution functions at front- and backside we conclude that the electron distribution is given by recirculation that acts effectively at our parameters. This is also supported by theory (Andreev *et al.*, 2009).

Furthermore, from the similar cut-off values of the backside ion spectra at mc and uhc similar maximum electron energy can be assumed. On the other hand, the different shape of these ion spectra is related to a change in the electron distribution function when the contrast of the laser pulse is altered. A change of the laser pulse contrast modifies the plasma gradient, which acts back to the absorption of the main laser pulse and the production of the energetic electrons building up the sheath field. Finally, the obtained experimental data serve as a benchmark for models that characterize the influence of the plasma gradient on the ion acceleration (Schnürer *et al.*, 2005; Sokollik *et al.*, 2010). Front and rear side symmetry of proton acceleration at uhc laser pulse conditions has been reported by Cecotti *et al.* (2007). Here we investigate this effect at an order higher laser intensities and down to an order thinner target foils as used in the work by Ceccoti *et al.* (2007). In difference to their conclusion, we do not observe that at our (higher) laser intensity the proton energies are "mostly related to the *p*-component of the laser electric field rather than to the ponderomotive potential" (Ceccoti *et al.*, 2007). We found highest proton energies at laser irradiation close to normal incidence when the *p*-component vanishes and we can assume that the ponderomotive potential as a function of laser intensity plays the dominant role at our parameter conditions.

The symmetric distribution of the circulating electrons between front and rear side of the target can be modified when the electro-magnetic field of the laser pulse interacts with the entire electron population in the focal volume i.e., if the target becomes transparent (Henig *et al.*, 2009*a*). In the case of relativistic intensities, the light pressure becomes high enough to modify the electron dynamics. This process

is even more effective when the light pressure dominates the thermal electron pressure. In our experiment, we reduced the thermal electron pressure by changing the laser polarization from linear to circular, which recently has led to the demonstration of radiation pressure acceleration (Henig *et al.*, 2009*b*). Figure 1 gives an indication on how the change of laser light polarization leads to a small but observable change in the cut-off energies of the protons. A slight increase of energies (Fig. 1b) of ions emitted from the target rear in comparison to target front side we attribute to an asymmetric electron distribution, which is governed by the light pressure. Still, the possibly observed effect is rather small at our conditions and has to be validated in future experiments. This is in principle a collective displacement of the major part of the electron ensemble (Yan *et al.*, 2008, 2010; Tajima *et al.*, 2009). In the following, we restrict the simple model analysis to data obtained at zero degree irradiation angle and linear laser polarization because this has resulted in the highest ion energies.

A simple model for maximum ion energies obtained from nanometer-thick targets

The electron energy is approximated by the hot electron temperature that is given by the ponderomotive potential of the laser field (kT_e — parameter in Eqs. (2)–(5) cf. the Appendix). Dissipation of electron energy, which is in principle cooling, is assumed to occur within a certain time interval on the order of four times the laser pulse duration (cf. Eq. (6) in the Appendix). This cooling results in the breakdown of the accelerating field and thus termination of ion acceleration. When the target foil thickness is decreased, a growing part of the bulk electrons can be pushed into the sheath at the target rear, because the laser starts to penetrate the entire target. At the optimum a maximum charge polarization of the target is realized and as mentioned above $a \sim n_e/n_c d_t/\lambda$ is achieved for the optimum thickness d_t. In our simple model, d_t is taken as a parameter for calculating this process (cf. Eq. (4) in the Appendix). Putting everything together, the target thickness, the Debye sheath extension (cf. Appendix), which is a function of the electron density and the electron energy, one arrives at an algebraic equation for the electron density. It is solved and then the sheath field strength and the ion acceleration within some time steps are calculated. The use of reasonable time steps is suggested by computer simulations, which are guides for typical acceleration durations at our laser parameters.

With variation of the parameters of the model, one can find quite reasonable measures and a good fit to the experimental data, which is shown in Figure 3. The experimental data has been obtained from DLC-foils irradiated with laser pulses at an intensity of 5×10^{19} W/cm^2 and an ultra-high temporal contrast. Here and in the following (Figs. 3, 4, 5), the laser irradiation is close to normal incidence. The experimentally observed peak can only be reproduced in its shape if a substantial part of the electrons are swept to the target rear,

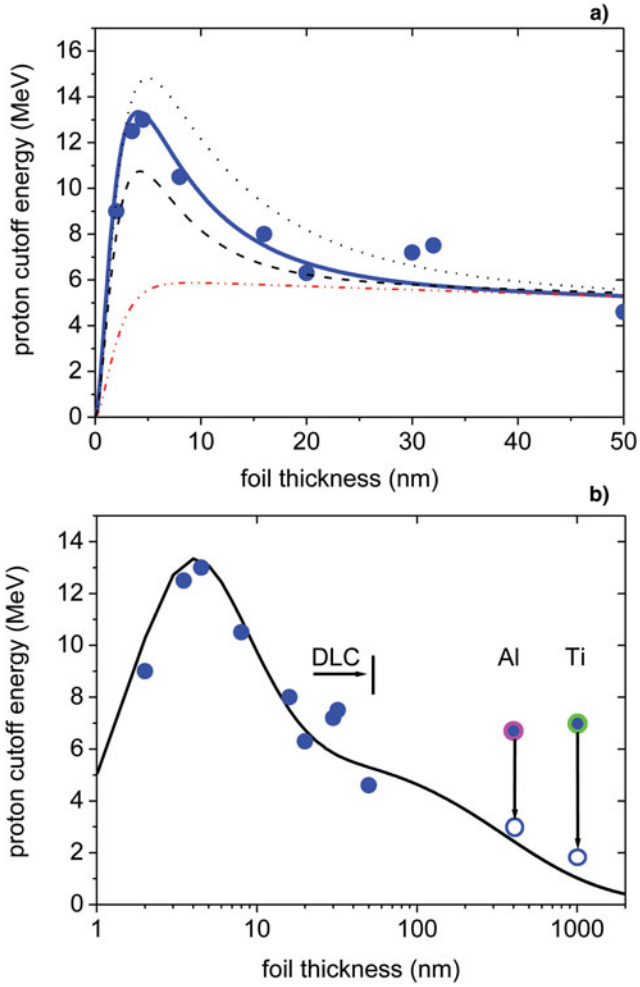

Fig. 3. (Color online) (**a**) maximum proton cut-off energies (blue dots) obtained from DLC-targets cf. (Steinke *et al.*, 2010) as a function of thickness and fit with a simple model function with parameter variation concerning interface polarization (solid versus dotted/dashed lines cf. text and appendix), laser with linear polarization at normal incidence and a peak intensity of 5×10^{19} W/cm^2; (**b**) same as (a) and data from two different metal foils and suggested *Z*-scaling (arrows to blue circles), all data points represent best (maximum) values — fluctuation due to shot variation is about 20%.

that is just what we specified as collective motion of the electrons in the field within a more comprehensive simulation, and real analytical models. Dotted and dashed lines give examples of higher and lower values (cf. Appendix) of the optimum thickness parameter that relates to higher and lower electron energies, respectively. If only electron circulation was driving the acceleration a smooth increase of proton energies peak values far below the observed ones would be expected (cf. Fig. 3 — low dotted/dashed line). If the foil thickness is reduced below the optimum, the balance condition of radiation and electrostatic pressure is not fulfilled anymore, and the electrons are able to escape the restoring field (Kiefer *et al.*, 2009).

Since the electron recirculation is still applicable for target thicknesses up to two orders of magnitude larger than in the DLC case discussed above (Andreev *et al.*, 2009), the models predictions in that regime are considered in the following.

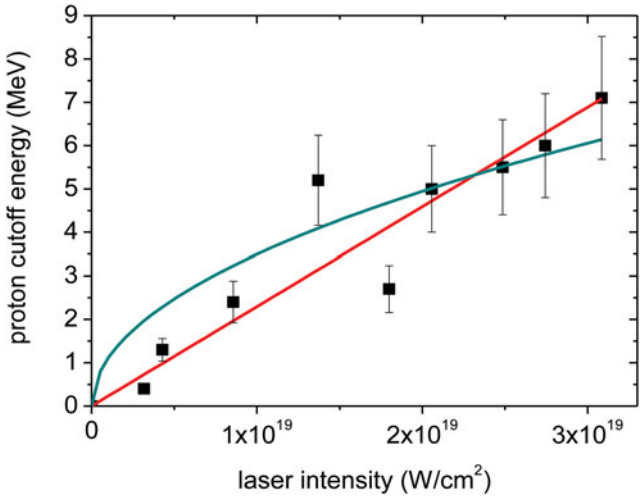

Fig. 4. (Color online) Proton cut-off energies obtained from irradiated 5 micrometer thick Ti-foils when the laser energy and thus the intensity was changed, linear and square root fits are included (black squares — laser beam close to 0° incident angle).

In Figure 3b, the model curve and obtained proton energies from a 400 nm thick Al-target as well as from a 1000 nm thick Ti-target are shown. For thick targets, the slope of our model curve indicates a scaling for the ion energies E_i as a function of the target thickness d_t that is about $E_i \sim d_t^{-0.8}$. This variation is much stronger as compared to $E_i \sim d_t^{-0.25}$, which one can reconstruct from equations of the adiabatic circulation model (Andreev *et al.*, 2009). If we would not regard the different atomic number (Z) — values of our target foils we could also infer a $E_i \sim d_t^{-0.2}$ scaling. In other experiments (Neely *et al.*, 2006; Cecotti *et al.*, 2007), a scaling behavior of $E_i \sim d_t^{-0.15--0.3}$ was measured when a target material with the same Z-number was used and the target thicknesses are within the validity range of the adiabatic circulation model. If we divide our experimental values of the maximum ion energy by the relative Z-values in comparison to carbon, that is 13/6 for Al and 22/6 for Ti, we arrive close to the proton energies extrapolated for the case of a DLC foil. Such a relatively strong dependence on the Z-number is suggested by analytical models (Andreev *et al.*, 2009). The role of the atomic number has been investigated in ion acceleration experiments (Badziak *et al.*, 2001) as well as in numerical simulations for the radiation pressure acceleration regime (Pae *et al.*, 2011) and its influence to the charge density has been suggested. Very recently Prasad *et al.* (2011) reported about a very weak dependence of ion energies on the target thickness when femtosecond laser pulses at very high intensities ($\sim 5 \times 10^{20}$ W/cm^2) were applied. This directs us to another mechanism that needs further exploration. Finally, the influence of the Z-number has to be analyzed in more detail when the target thickness is varied up to three orders of magnitude. The indications of a favorable influence of the Z-number on the achievable ion energies leads to the interpretation of another scaling experiment which is discussed in the next paragraph.

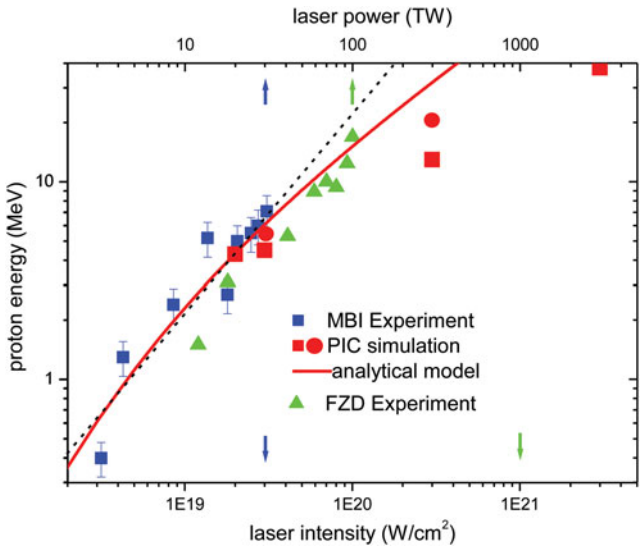

Fig. 5. (Color online) Dependence of maximal proton energy on laser intensity and power. Blue squares are experimental data from this work concerning intensity and power, green triangles are experimental data from Zeil *et al.* (2010) scaled *via* laser power (pulse duration of the Draco-laser at FZD is about 50% of the HFL-laser at MBI), red square are two-dimensional PIC simulation result for Ti-foil targets (parameter cf. text) red solid line is the analytical model (parameter cf. text). Blue (MBI-experiment) and green (FZD-experiment) arrows indicate the relation between laser power and intensity.

SCALING OF PROTON ENERGIES AS A FUNCTION OF LASER DRIVER ENERGY IN CASE OF ULTRA-SHORT LASER PULSES WITH HIGH TEMPORAL CONTRAST

If the intensity in the pedestal of the laser pulse reaches a level of about 10^{11}–10^{12} W/cm^2 during a temporal window of several 100 ps, the ionization threshold of a metal surface is exceeded and a pre-plasma is formed. Plasma expansion and ion acceleration at very low laser intensities has been exemplified recently (Torrisi *et al.*, 2011). Such pulse parameters are typical for a about 10^{10}-fold amplification of laser pulses if no additional device for temporal pulse cleaning is applied. Such a pre-plasma does not only disrupt the steep density gradient at the target front side, but it can influence the density gradient at the target rear side due to launched heat (Badziak *et al.*, 2002) and shock waves (Lundh *et al.*, 2007). Because the acceleration of ions at the target rear side is triggered by fast electrons, the target thickness has to be adjusted such that the arrival of the slower, but due to the pre-pulse earlier initiated perturbation, waves occurs after the termination of the ion acceleration. For our experimental laser parameter (mc), this is usually fulfilled if target foils on the order of about μm in thickness are used. Even if such a target system cannot provide the record ion energy values attainable with ultra-thin foils, they are of interest for practical applications as they offer robust and cheap solutions for a high repetition rate laser driven source. Furthermore, a broader variety of materials with different atomic numbers is available.

Gathering ion acceleration results from different ultrafast laser systems indicates that the scaling of ion energy with laser energy and intensity might be different than the usual predictions of the TNSA-model (Nickles *et al.*, 2008). With the presently available laser parameters, we could now perform an useful scaling experiment. Changing the laser energy over one order of magnitude should provide some significance for a certain scaling function.

The experiments have been conducted with 5 μm thick Ti-foils and the obtained maximum proton energies are plotted in Figure 4. The intensity of the pulse pedestal was about 10^{-7}–10^{-8} of the peak of the pulse (mc). The data suggest that a linear increase of the ion energy with laser energy fits much better compared to a square root dependence. The TNSA-model predicts a scaling $W_{ion} \sim (kT_e n_{eff})^{1/2}$ for the ion energy W_{ion} as a function of the electron energy kT_e and the electron density n_{eff}. The energy of the laser heated electrons is proportional to the laser intensity $kT_e \sim (\text{const.} + I_L)^{1/2}$ (e.g., Andreev *et al.* (2009)). In case of targets with a low atomic number, the ionization saturates at laser intensities of 10^{18}–10^{19} W/cm^2 and the electron density does not change significantly over the intensity range studied in our measurement. This situation changes when elements with higher atomic number are irradiated. In case of Ti, a simple approximation of the ionization appearance intensity (Augst *et al.*, 1991) leads to a functional dependence of about $n_e \sim I_L^{0.6}$ if the laser intensity varies between 8×10^{18}–3×10^{19} W/cm^2. The number of ionized electrons increases with the degree of ionization from 13 and 20 over this intensity range. This can explain a deviation from the square root scaling in ion energy. Recently Zeil *et al.* (2010) proposed an interpretation of the TNSA model by Schreiber *et al.* (2006), which shows that in a certain parameter range and in the case of ultra-short laser pulses, a linear scaling between ion energy and laser energy is feasible. In order to study this complex scenario more thoroughly, an analytical model has been developed and computer simulations have been carried out.

SIMULATION OF PROTON ENERGIES OBTAINED WITH MICROMETER-THICK TI-FOILS

The interaction of the laser pulse with a plasma target was simulated with a special PIC code (Andreev *et al.*, 2009). The two-dimensional version of the code was used because it accounts for important effects such as the influence of the magnetic field on the electrons or the lateral propagation of fast electron along the target rear surface. The simulations were performed for a laser wavelengths of $\lambda_L = 0.8$ μm and for different laser intensities between 2×10^{19} W/cm^2 and 3×10^{21} W/cm^2. The irradiation was approximated with a temporal Gaussian pulse shape with a half-width of $t_L =$ 45 fs and a super-Gaussian beam spot radius of $r_L = 3\lambda_L$ at normal incidence on the foil. In the case of two-dimensional simulations, we were using a spatial domain of 50 μm along the laser direction z and 30 μm in the transverse direction y. The spatial grid size was 10 nm. In our simulations, the number of particles per cell was five for any particle species. The boundary conditions in our simulation are as follows: the electromagnetic field propagates through the boundary without reflection or absorption and the boundary for particles in lateral direction is periodical (particles leaving through one boundary appear at the opposite one) and in laser propagation direction the extension is matched to the simulation time. Taking the ultra-short duration of the laser pulse into consideration, the ion charge Z of the Ti-atoms in the target foil was calculated with tunnel ionization rates of the target atom in the electric field of the laser pulse and the sheath field at the target rear. The results of the simulations are shown in the Figure 5. To account for the different laser intensities, we adjust the ionization state of the Ti for each intensity (cf. Fig. 5: $Z = 10$ — red squares, $Z = 16$ and $Z = 20$ — red dots).

When the plasma mirror is not used, the contrast value of the laser pulse provides an estimate of the initial plasma density scale length at about 400 nm and 600 nm for higher intensities, respectively. The target foil is covered with a thin layer of hydrogen-containing molecules. For computational reasons, PIC simulations have been carried out with a layer of 50 nm hydrogen while a density of 25% of solid hydrogen was applied.

For interpretation of the experimental data, an analytical model was developed. The temporal evolution of the electron and the following ion distribution functions is calculated with a one-dimensional hybrid isothermal-adiabatic model (Andreev *et al.*, 2011). The distribution of the heavy ions is described with a rectangular step function having a varying width (target thickness) and the distribution of the thin contaminant hydrogen layer is a δ-function. The equations for the acceleration of ions are the Poisson equation for the evolving electric field and the equations of motion for velocity calculation of the light and heavy ion front. The details of the model will be published elsewhere (Andreev *et al.*, 2011). After all the dependence of the maximum proton energy on both, the initial foil and laser pulse parameters can be described by the following formula:

$$\varepsilon_p \approx 0.6 m_e c^2 (\gamma - 1) \ln(1 + 1.2/\xi + 3/\xi^2), \qquad (1)$$

where $\xi = 2\pi Z_1 n_{i1} l_{i1}/\lambda (\gamma - 1) \sqrt{Z_2 n_{i2} n_c}$, l_{i1} — proton layer thickness, Z_j — ion charge, n_{ij} — ion density (with $j =$ 1— hydrogen, 2 — heavy ions), n_c — electron critical density, $\gamma = \sqrt{1 + a^2}$ and a is the laser vector potential.

Eq. (1) is based on energy conservation and the assumption that fast electrons are circulating through the foil. It is obvious from Eq. (1) that for $\xi < 1$ the proton energy increases almost linearly with the laser intensity (cf. comparison with dashed line in Fig. 5). In principle, we can regard the parameter ξ as an effective steering function that accounts for the charge densities of the target subjected to the laser intensity. If the laser intensity grows and the target ionization saturates, the parameter turns to $\xi > 1$ and the proton energy

increases with the square root of the laser intensity. This reflects the behavior of the standard TNSA-model. The formula given above can be applied for the interpretation of experimental data until ultra-relativistic laser intensities ($>10^{21}$ W/cm^2) are reached. At higher intensities multi-dimensional effects should be taken into account. For comparison with the experiment we used:

$$n_c = 1.5 \cdot 10^{21} cm^{-3},\ n_{i2} = 6 \cdot 10^{22} cm^{-3},\ n_{i1} = 2 \cdot 10^{22} cm^{-3},\ l_{i1} = 50\ nm,\ Z_2 = 10,\ Z_1 = 1$$

As visible in Figure 5, a quiet reasonable description of our data and those of Zeil *et al.* (2010) is achieved for the Ti-target foils with thicknesses of a few microns used in the experiments.

CONCLUSION

In order to approach the limits of the target normal acceleration scheme, laser and target parameters have to be found that maximize the electron density in the sheath layer and account for a maximum polarization at the plasma vacuum interface. Experiments and elaborate theoretical studies have shown that such a situation can be achieved with targets of nanometer thickness if the laser intensity becomes relativistic and the light pressure starts to influence the scenario. This situation was approximated by model functions that are able to reproduce the measured cut-off ion energies as function of the target thickness. Another potential of optimization is related to the ionization of the target material. Targets with a high atomic number can provide higher electron densities which seem to pay off especially if ultra-short laser pulses are used to create the sheath field. This situation has been investigated and an almost linear scaling of the cut-off ion energies as a function of the laser energy was found.

ACKNOWLEDGMENTS

This work was partly supported by Deutsche Forschungsgemeinschaft through Transregio SFB TR18. This research was supported by a Marie Curie International Incoming Fellowship (No. PIIF-GA-2008-221727) within the 7th European Community Framework Programme. P.V.N. acknowledges the support of World Class University program (R31-2008-000-10026-0) grant provided by NRF of Korea.

REFERENCES

Andreev, A.A., Steinke, S., Sokollik, T., Schnurer, M., Ter Avetsiyan, S., Platonov, K.Y. & Nickles, P.V. (2009). Optimal ion acceleration from ultrathin foils irradiated by a profiled laser pulse of relativistic intensity. *Phys. Plasmas* **16**, 013103.

Andreev, A.A. & Platonov, K.V. (2011). Hybrid model of ion acceleration in laser plasma of flat heterogeneous target. *Opt. Spectr.* **111**, 191–199.

Andreev, A.A., Steinke, S., Schnuerer, M., Henig, A., Nickles, P.V., Platonov, K.Y., Sokolik, T. & Sandner, W. (2010). Hybrid ion acceleration with ultrathin composite foils irradiated by high intensity circularly-polarized laser light. *Phys. Plasmas* **17**, 123111.

Augst, S., Meyerhofer, D.D., Strickland, D. & Chin, S.L. (1991). Laser ionization of noble-gases by coulomb-barrier suppression. *J. Opt. Soc. Am. B* **8**, 858–867.

Badziak, J., Woryna, E., Parys, P., Platonov, K.Y., Jablonski, S., Ryc, L.,Vankov, A.B. & Wolowski, J. (2001). Fast proton generation from ultrashort laser pulse interaction with double-layer foil targets. *Phys. Rev. Lett.* **87**, 215001/1–4.

Badziak, J., Woryna, E., Parys, P., Wolowski, J., Platonov, K.Y. & Vankov, A.B. (2002). Effect of foil target thickness on fast proton generation driven by ultrashort-pulse laser. *J. Appl. Phys.* **91**, 5504–5506.

Badziak, J., Jablonski, S., Parys, P., Szydlowski, A., Fuchs, J. & Mancic, A. (2010). Production of high-intensity proton fluxes by a 2ω Nd:glass laser beam. *Laser Part. Beams* **28**, 575–583.

Brenner, C.M., Green, J.S., Robinson, A.P.L., Carroll, D.C., Dromey, B., Foster, P.S., Kar, S., Li, Y.T., Markey, K., Spindloe, C., Streeter, M.J.V., Tolley, M., Wahlström, C.-G., Xu, M.H., Zepf, M., McKenna, P. & Neely, D. (2011). Dependence of laser accelerated protons on laser energy following the interaction of defocused, intense laser pulses with ultra-thin targets. *Laser Part. Beams* **29**, 345–351.

Borghesi, M., Audebert, P., Bulanov, S.V., Cowan, T., Fuchs, J., Gauthier, J.C., Mackinnon, A.J., Patel, P.K., Pretzler, G., Romagnani, L., Schiavi, A., Toncian, T. & Willi, O. (2005). High-intensity laser-plasma interaction studies employing laser-driven proton probes. *Laser Part. Beams* **23**, 291–295.

Ceccotti, T., Levy, A., Popescu, H., Reau, F., D'oliveira, P., Monot, P., Geindre, J.P., Lefebvre, E. & Martin, P. (2007). Proton acceleration with high-intensity ultrahigh-contrast laser pulses. *Phys. Rev. Lett.* **99**, 185002.

Cowan, T.E., Fuchs, J., Ruhl, H., Kemp, A., Audebert, P., Roth, M., Stephens, R., Barton, I., Blazevic, A., Brambrink, E., Cobble, J., Fernandez, J., Gauthier, J.C., Geissel, M., Hegelich, M., Kaae, J., Karsch, S., Le Sage, G.P., Letzring, S., Manclossi, M., Meyroneinc, S., Newkirk, A., Pepin, H. & Renard-Legalloudec, N. (2004). Ultralow emittance, multi-MeV proton beams from a laser virtual-cathode plasma accelerator. *Phys. Rev. Lett.* **92**, 204801.

Esirkepov, T., Yamagiwa, M. & Tajima, T. (2006). Laser ion-acceleration scaling laws seen in multiparametric particle-in-cell simulations. *Phys. Rev. Lett.* **96**, 105001.

Flacco, A., Cecotti, T., George, H., Monot, P., Martin, Ph., Réau, F.,Tscherbakoff, O., D'Oliveira, P., Sylla, F., Veltcheva, M., Burgy, F., Tafzi, A.,Malka, V. & Batani, D. (2010). Comparative study of laser ion acceleration with different contrast enhancement techniques. *Nucl. Instrum. Meth. Phys. Res. A* **620**, 18–22.

Hatchett, S.P., Brown, C.G., Cowan, T.E., Henry, E.A., Johnson, J.S., Key, M.H., Koch, J.A., Langdon, A.B., Lasinski, B.F., Lee, R.W., Mackinnon, A.J., Pennington, D.M., Perry, M.D., Phillips, T.W., Roth, M., Sangster, T.C., Singh, M.S., Snavely, R.A., Stoyer, M.A., Wilks, S.C. & Yasuike, K. (2000). Electron, photon, and ion beams from the relativistic interaction of Petawatt laser pulses with solid targets. *Phys. Plasmas* **7**, 2076–2082.

Henig, A., Kiefer, D., Markey, K., Gauthier, D.C., Flippo, K.A., Letzring, S., Johnson, R.P., Shimada, T., Yin, L., Albright, B.J., Bowers, K.J., Fernandez, J.C., Rykovanov, S.G., Wu,

W.C., Zepf, M., Jung, D., Liechtenstein, V.Kh., Schreiber, J., Habs, D. & Hegelich, B.M. (2009*a*). Enhanced laser-driven ion acceleration in the relativistic transparency regime. *Phys. Rev. Lett.* **103**, 045002.

Henig, A., Steinke, S., Schnurer, M., Sokollik, T., Horlein, R., Kiefer, D., Jung, D., Schreiber, J., Hegelich, B.M., Yan, X.Q., Meyer-Ter-Vehn, J., Tajima, T., Nickles, P.V., Sandner, W. & Habs, D. (2009*b*). Radiation-pressure acceleration of ion beams driven by circularly polarized laser pulses. *Phys. Rev. Lett.* **103**, 245003.

Kaluza, M., Schreiber, J., Santala, M.I.K., Tsakiris, G.D., Eidmann, K., Meyer-Ter-Vehn, J. & Witte, K.J. (2004). Influence of the laser prepulse on proton acceleration in thin-foil experiments. *Phys. Rev. Lett.* **93**, 045003.

Kiefer, D., Henig, A., Jung, D., Gautier, D.C., Flippo, K.A., Gaillard, S.A., Letzring, S., Johnson, R., Shah, R.C., Shimada, T., Fernández, J.C., Liechtenstein, V.Kh., Schreiber, J., Hegelich, B.M. & Habs, D. (2009). First observation of quasi-monoenergetic electron bunches driven out of ultra-thin diamond-like carbon (DLC) foils. *Euro. Phys. J. D* **55**, 427.

Klimo, O., Psikal, J., Limpouch, J. & Tikhonchuk, V.T. (2008). Monoenergetic ion beams from ultrathin foils irradiated by ultrahigh-contrast circularly polarized laser pulses. *Phys. Rev.* **11**, 031301.

Kraft, S.D., Richter, C., Zeil, K., Baumann, M., Beyreuther, E., Bock, S., Busmann, M., Cowan, T.E., Dammene, Y., Enghardt, W., Helbig, U., Karsch, L. Kluge, T., Laschinsky, L., Lessmann, E., Metzkes, J., Naumburger, D., Sauerbrey, R., Schürer, M., Sobiella, M., Woithe, J., Schramm, U. & Pawelke, J. (2010). Dose-dependent biological damage of tumor cells by laser-accelerated proton beams. *New J. Phys.* **12**, 085003.

Levy, A., Ceccotti, T., D'oliveira, P., Reau, F., Perdrix, M., Quere, F., Monot, P., Bougeard, M., Lagadec, H., Martin, P., Geindre, J.P. & Audebert, P. (2007). Double plasma mirror for ultrahigh temporal contrast ultraintense laser pulses. *Opt. Lett.* **32**, 310–312.

Lundh, O., Lindau, F., Persson, A., Wahlstrom, C.G., Mckenna, P. & Batani, D. (2007). Influence of shock waves on laser-driven proton acceleration. *Phys. Rev. E* **76**, 26404.

MaCchi, A., Veghini, S. & Pegoraro, F. (2009). "Light sail" acceleration reexamined. *Phys. Rev. Lett.* **103**, 085003.

MaCchi, A., Veghini, S., Liseykina, T.V. & Pegoraro, F. (2009). Radiation pressure acceleration of ultrathin foils. *New J. Phys.* **12**, 045013.

Mackinnon, A.J., Patel, P.K., Town, R.P., Edwards, M.J., Phillips, T., Lerner, S.C., Price, D.W., Hicks, D., Key, M.H., Hatchett, S., Wilks, S.C., Borghesi, M., Romagnani, L., Kar, S., Toncian, T., Pretzler, G., Willi, O., Koenig, M., Martinolli, E., Lepape, S., Benuzzi-Mounaix, A., Audebert, P., Gauthier, J.C., King, J., Snavely, R., Freeman, R.R. & Boehlly, T. (2004). Proton radiography as an electromagnetic field and density perturbation diagnostic (invited). *Rev. Sci. Instr.* **75**, 3531–3536.

Mckenna, P., Carroll, D.C., Lundh, O., Nürnberg, F., Markev, K., Bandyopadhyay, S., Batani, D., Evans, R.G., Jafer, R., Kar, S., Neely, D., Pepler, D., Quinn, M.N., Redaelli, R., Roth, M., Wahlström, C.G., Yuan, X.H. & Zepf, M. (2008). Effects of front surface plasma expansion on proton acceleration in ultraintense laser irradiation of foil targets. *Laser Part. Beams* **26**, 591–596.

Neely, D., Foster, P., Robinson, A., Lindau, F., Lundh, O., Persson, A., Wahlstrom, C.G. & Mckenna, P. (2006). Enhanced proton beams from ultrathin targets driven by high contrast laser pulses. *Appl. Phys. Lett.* **89**, 021502.

Nickles, P.V., Schnurer, M., Sokollik, T., Ter-Avetisyan, S., Sandner, W., Amin, M., Toncian, T., Willi, O. & Andreev, A. (2008). Ultrafast laser-driven proton sources and dynamic proton imaging. *J. Opt. Soc. Am. B* **25**, B155–B160.

Pae, K.H., Choi, I. W. & Lee, J. (2011). Effect of target composition on proton acceleration by intense laser pulses in the radiation pressure regime, *Laser Part. Beams* **29**, 11–16.

Prasad, R., Ter-Avetisyan, S., Doria, D., Quinn, K.E., Romagnani, L, Foster, P.S., Brenner, C.M., Green, J.S., Gallegos, P, Streeter, M.J.V., Carroll, D.C., Tresca, O., Dover, N.P., Palmer, C.A.J., Schreiber, J., Neely, D., Najmudin, Z., Mckenna, P., Zepf, M. & Borghesi, M. (2011). Proton acceleration using 50 fs, high intensity ASTRA-Gemini laser pulses, *Nucl. Instrum. Phys. Res. A* doi:10.1016/j.nima.2011.01.021.

Romagnani, L., Fuchs, J., Borghesi, M., Antici, P., Audebert, P., Ceccherini, F., Cowan, T., Grismayer, T., Kar, S., Macchi, A., Mora, P., Pretzler, G., Schiavi, A., Toncian, T. & Willi, O. (2005). Dynamics of electric fields driving the laser acceleration of multi-MeV protons. *Phys. Rev. Lett.* **95**, 195001.

Schnurer, M., Ter-Avetisyan, S., Busch, S., Risse, E., Kalachnikov, M.P., Sandner, W. & Nickles, P. (2005). Ion acceleration with ultrafast laser driven water droplets. *Laser Part. Beams* **23**, 337–343.

Schreiber, J., Bell, F., Grüner, F., Schramm, U., Geissler, M., Schnürer, M., Ter-Avetisyan, S., Hegelich, B.M, Cobble, J., Brambrink, E., Fuchs, J., Audebert, P. & Habs D. (2006). Analytical model for ion acceleration by high-intensity laser pulses. *Phys. Rev. Lett.* **97**, 045005.

Sokollik, T., Schnurer, M., Steinke, S., Nickles, P.V., Sandner, W., Amin, M., Toncian, T., Willi, O. & Andreev, A.A. (2009). Directional laser-driven ion acceleration from microspheres. *Phys. Rev. Lett.* **103**, 135003.

Sokollik, T., Paasch-Colberg, Gorling, K., Eichmann, U., Schnurer, M., Steinke, S., Nickles, P.V., Andreev, A.A. & Sandner, W. (2010). Laser driven ion acceleration using mass-limited targets. *New J. Phys.* **12**, 113013.

Steinke, S., Henig, A., Schnurer, M., Sokollik, T., Nickles, P.V., Jung, D., Kiefer, D., Horlein, R., Schreiber, J., Tajima, T., Yan, X.Q., Hegelich, M., Meyer-Ter-Vehn, J., Sandner, W. & Habs, D. (2010). Efficient ion acceleration by collective laser-driven electron dynamics with ultra-thin foil targets. *Laser Part. Beams* **28**, 215–221.

Steinke, S., Schnurer, M., Sokollik, T., Andreev, A.A., Nickles, P.V., Henig, A., Horlein, R., Kiefer, D., Jung, D., Schreiber, J., Tajima, T., Hegelich, M., Habs, D. & Sandner, W. (2011). Optimization of laser-generated ion beams. *Conrib. Plasma Phys.* **51**, 444–450.

Tajima, T., Habs, D. & Yan, X.Q. (2009). Laser acceleration of ions for radiation therapy. *Rev. Acc. Sci. Technol.* **2**, 201–228.

Ter-Avetisyan, S., Schnurer, M. & Nickles, P.V. (2005). Time resolved corpuscular diagnostics of plasmas produced with high-intensity femtosecond laser pulses. *J. Phys. D* **38**, 863–867.

Torrisi, L., Caridi, F. & Giuffrida, L. (2011). Protons and ion acceleration from thick targets at 10^{10} W/cm^2 laser pulse intensity. *Laser Part. Beams* **29**, 29–37.

Weichsel, J., Fuchs, T., Lefebvre, E., D'humieres, E. & Oelfke, U. (2008). Spectral features of laser-accelerated protons for radiotherapy applications. *Phys. Med. Bio.***53**, 4383–4397.

Willingale, L., Nilson, P.M., Kaluza, M.C., Dangor, A.E., Evans, R.G., Fernandes, P., Haines, M.G., Kamperidis, C., Kingham, R.J., Ridgers, C.P., Sherlock, M., Thomas, A.G.R., Wei, M.S., Najmudin, Z., Krushelnick, K., Bandyopadhyay, S., Notley, M., Minardi, S., Tatarakis, M. & Rozmus, W. (2010). Proton deflectometry of a magnetic reconnection geometry. *Phys. Plasmas* **17**, 043104.

Yan, X.Q., Lin, C., Sheng, Z.M., Guo, Z.Y., Liu, B.C., Lu, Y.R., Fang, J.X. & Chen, J.E. (2008). Generating high-current monoenergetic proton beams by a circularly polarized laser pulse in the phase-stable acceleration regime. *Phys. Rev. Lett* **100**, 135003.

Yan, X.Q., Tajima, T., Hegelich, M., Yin, L. & Habs, D. (2010). Theory of laser ion acceleration from a foil target of nanometer thickness. *Appl. Phys. B* **98**, 711–721.

Zeil, K., Kraft, S.D., Bock, S., Bussmann, M., Cowan, T.E., Kluge, T., Metzkes, J., Richter, T., Sauerbrey, R. & Schramm, U. (2010). The scaling of proton energies in ultrashort pulse laser plasma acceleration. *New J. Phys.* **12**, 045015.

APPENDIX

The laser irradiates an area A and ionizes the target material within its penetration depth d_{skin}. Using the ion density n_i and an effective ionization state Z_{eff}, we write the generated electron number $N_e(d_t)$ in the form

$$N_e(d_t) = (d_{skin} - d_{skin}(\exp((-d_t/d_{skin})^2)))A\, Z_{eff}\, n_i, \qquad \text{(A1)}$$

with d_t — the thickness of the target foil. (A1) specifically accounts for a functional dependence of the electron density if the thickness of the target foil becomes comparable to the effective laser penetration depth (or skin layer, the deviation to the classical skin layer at relativistic laser intensities is shown in Steinke *et al*. (2010)). The skin depth parameter describes the decline of the electrical field in matter and electron generation by field ionization is a non-linear function of the field strength. Both together give a complex relation that we approximate with a simple electron number function (A1). For model calculation, we tested a linear and a quadratic exponential expression. The latter one gave better results and has been used for the model function. We describe the electron distribution function with a kT_e parameter that is in the order of the ponderomotive potential of the focused laser pulse. In the parameter range of interest for our experiments, we can use the electron circulation scenario (Andreev *et al*., 2009) that means the electrons fill the two electron sheath regions (each with an extension of λ_D) at the target front and rear as well as the extent of the target in between. The volume of this total region is calculated assuming a cylinder of cross-section A and a length of $2\lambda_D + d_t$. The filling of this volume with the produced electrons leads to an effective electron density $n_{eff\ circ}$. We associate λ_D with the Debye length:

$$\lambda_D = \mathrm{con}(kT_e)(1/n_{eff\ circ})^{1/2}; \quad \mathrm{con}(kT_e) = (\varepsilon_0 kT_e/e_0^2)^{1/2}, \qquad \text{(A2)}$$

ε_0 and e_0 are the vacuum permeability and the elementary charge, respectively. The calculation of $n_{eff}(d_t)$ with $n_{eff\ cic}(d_t) = N_{e\ circ}(d_t)/(A(2\lambda_D + d_t))$ leads to:

$$n_{eff\ circ}(d_t) = N_{e\,circ}(d_t)/(A(2\,\mathrm{con}(kT_e)(1/n_{eff\ circ})^{1/2} + d_t)) \qquad \text{(A3)}$$

an algebraic equation that can be solved for $n_{eff\ circ}(d_t)$.

As the laser starts to penetrate the thin target foil, the number of circulating electrons $N_{e\ circ}$ is reduced and an increasing number of electrons are pushed to the target rear side until a maximum polarization as a function of laser intensity is reached. This condition can be described with an optimum foil thickness parameter d_{opt} (cf. discussion in text). If the thickness of the target is smaller as the optimum thickness, the electrical field of the target charge can not compensate the light pressure any longer. Therefore, electrons are blown out. This process has been approximated with an exponential function for the electron density. In order to calculate the ratio of electrons $N_{e\ fw} = N_e - N_{e\ circ}$, which is influenced by this process if one approaches the relevant target extension, we set:

$$\begin{aligned} N_{e\,fw}(d_t) &= N_e(d_t)\exp(-d_t/d_{opt}); \\ n_{eff\,fw}(d_t) &= N_{e\,fw}(d_t)/(\mathrm{A\ con}(kT_e)(1/n_{eff\,fw}(d_t))^{1/2}. \end{aligned} \qquad \text{(A4)}$$

With (A3) and (A4) we can calculate for the target rear $n_{eff} = n_{eff\ fw} + n_{eff\ cric}$ and use

$$E_{field} = (kT_e n_{eff}/\varepsilon_0)^{1/2} \qquad \text{(A5)}$$

in order to calculate the strength of the acceleration field. The action of this field within a certain time step Δt leads to acceleration and a certain velocity (the kinetic energy of protons ($Z = 1$) is $1/2e_0^2 E_{field}^2/m_{ion}\Delta t^2$). Furthermore we consider that the electron energy decreases with time:

$$kT_e \sim kT_{e0}\,(\Delta t_0/\Delta t)^2 \qquad \text{(A6)}$$

(cf. remark in discussion) in which we approximate Δt with discrete time steps at the order of Δt_0. Also the process of electron density enhancement in forward direction is switched off with a step function if the laser pulse is off. All equations, algebraic solutions and conditions are put together in a small programme which yields ion energies as a function of the used parameter. The blue-solid curve plotted in Figure 3a has been obtained with the following parameter set:

$$\begin{gathered} d_{skin} = 3.5\,\mathrm{nm},\ A = 10\,\mu\mathrm{m}^2,\ Z_{eff}\, n_i = 6\times 10^{23}\,\mathrm{cm}^{-3}, \\ kT_e = 1.2\,\mathrm{MeV},\ d_{opt} = 8\,\mathrm{nm},\ \Delta_0 t = 21\,\mathrm{fs}; \end{gathered}$$

Parameter variations result in dotted ($kT_e = 0.6$ MeV, $d_{opt} = 5.7$ nm) and dashed ($kT_e = 2.4$ MeV, $d_{opt} = 11.3$ nm) black curves.